PROCEEDINGS OF THE SEVENTH INTERNATIONAL CONFERENCE ON VEHICLE STRUCTURAL MECHANICS

P-210

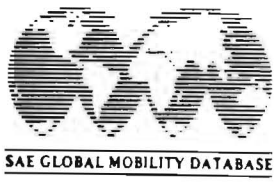

The papers included in this volume are abstracted and indexed in the SAE Global Mobility Database

Published by:
Society of Automotive Engineers, Inc.
400 Commonwealth Drive
Warrendale, PA 15096-0001
April 1988

880472PG:27

880892

Structural Adhesive Joints for Application to a Composite Space Frame — Analysis and Testing

Nancy L. Johnson and George A. Kardomateas
Engineering Mechanics Dept.
General Motors Research Labs.

ABSTRACT

This paper presents an efficient adhesively bonded joint design for application to a composite space frame. After preliminary investigations were conducted to evaluate several alternative joint configurations, an adhesively bonded insert type T-joint was chosen for use in a composite space frame because of its high specific stiffness and large bond area. The stiffnesses of each joint were investigated both analytically and experimentally. Since the lower rail is the primary load bearing member, the joints along it were selected for a detailed study. Two types of analyses were completed. First, a formulation based on the layered beam concept and strain energy theorems was used as an approximate measure to evaluate the effects of varying geometrical parameters. The relationships between joint flange width, insert thickness, and weight were considered. Using the geometry determined by the approximate formulation, a finite element analysis was completed. The finite element model itself consisted of approximately 2800 solid isoparametric elements. All of the materials were modeled including the adhesive layer. The details of the two analysis techniques are presented in this paper.

Bending tests were used to verify the joint stiffnesses obtained. Three specimens were tested for each of the three joints considered under both fore-aft and vertical loading. The displacements were measured at the free end of the cross member where the load was applied.

COMPOSITE MATERIALS and structural adhesive bonding have been used by the aerospace industry for many years. With the interest in applying composite materials to primary automotive structural components, the necessity of investigating adhesively bonded joints has increased. Designing an adhesive joint presents more challenges than designing joints using traditional elastic materials. Adams and Wake (1)* point out some of these difficulties in their consideration of various adhesive joint geometries. Much progress has been made to assist in choosing an adhesive system. However, difficulties still remain. The material properties of the adhesive layer necessary for the analysis are difficult to acquire. Thickness of the adhesive and the surface area of the bond become variables to be carefully investigated.

The present paper deals with the design of adhesively bonded joints for a composite space frame shown in Figure 1. The frame is manufactured using Kevlar**/epoxy for all parts except the tunnel which is graphite/epoxy. Kevlar was chosen because of its high energy absorption capability (2). Many types of joints were considered for the frame, and different joining materials were also evaluated.

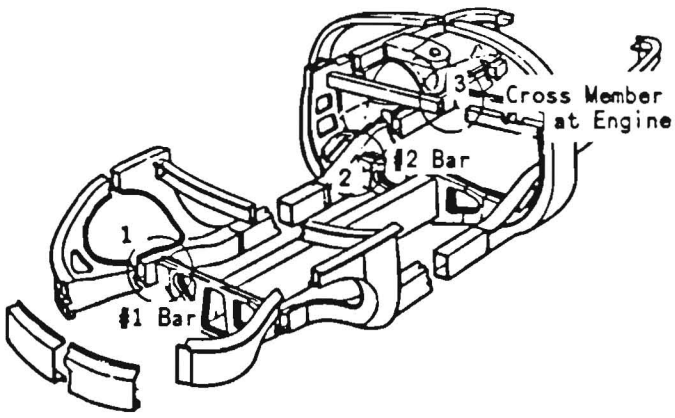

Fig. 1 - Locations of Joints Evaluated

*Numbers in parentheses designate references at end of paper.

**Kevlar is a registered trademark of Du Pont, Inc.

The following sections of the paper discuss the determination of joint design and material selection, present the two analytical techniques used, and describe the experimental procedure. The results from each method are then compared.

JOINT SELECTION

A joint design was needed which had a large bond area to provide a fairly uniform stress distribution and which had a stiffness at least that of a corresponding steel joint. The insert type T-joint shown in Figure 2 satisfied these criteria. The insert is bonded to the lower rail on the top, bottom, and back faces as well as along the flanges. The cross member is bonded to the aluminum on all four sides.

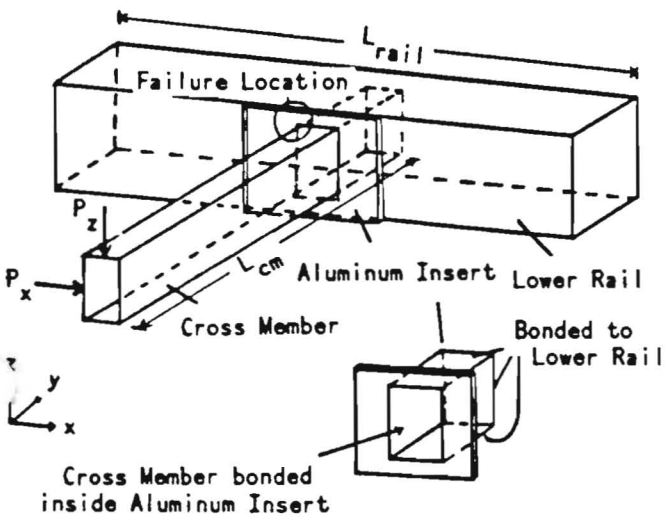

Fig. 2 - T-Joint Geometry

Different materials were considered for the insert. Aluminum was chosen due to material availability and ease of fabrication. Other materials of even less weight could have been used. Due to the various dimensions of the rails in the frame, the actual dimensions varied for each joint. The locations in the space frame of each joint which was evaluated are circled in Figure 1.

ANALYSIS APPROACH

ANALYSIS TECHNIQUES - Initially, an approximate formulation based on the layered beam concept was used to size the joint. It accounts for the variation of materials through the thickness. Stiffness is determined by integration over the length and across the thickness. Once an approximate design was chosen, a finite element analysis was done to obtain more detailed information about the joint.

APPROXIMATE FORMULATION - The formulation is based on the layered beam concept. The configuration being considered has cross sections that consist of layers of different material. As shown in Figure 3, section I consists of the inner composite rail (C1), the adhesive layer between the inner rail and the insert (A1), the metal insert (M1), and the outer composite rail (C2). Section II consists of the adhesive layer around the inner rail end section (A3), the insert (M1), and the outer composite rail (C2). Section III consists of the metal insert (M2) and the outer composite rail (C2). Section IV consists of the back adhesive layer (A2) and the outer composite rail (C2). Section V consists of the composite back face (C3), while section VI consists of the inner composite rail (C1), the adhesive layer between the inner rail and the insert (A1), and the metal flange (M3). Section VII is made of the inner composite rail (C1), the adhesive layer between the inner rail and the insert (A1), the metal insert (M1), and the adhesive layer between the flange and outer rail (A4). Finally, section VIII consists of the inner composite rail (C1), the adhesive layer between the inner rail and the insert (A1), the metal insert (M1), and the side walls of the outer rail (C4).

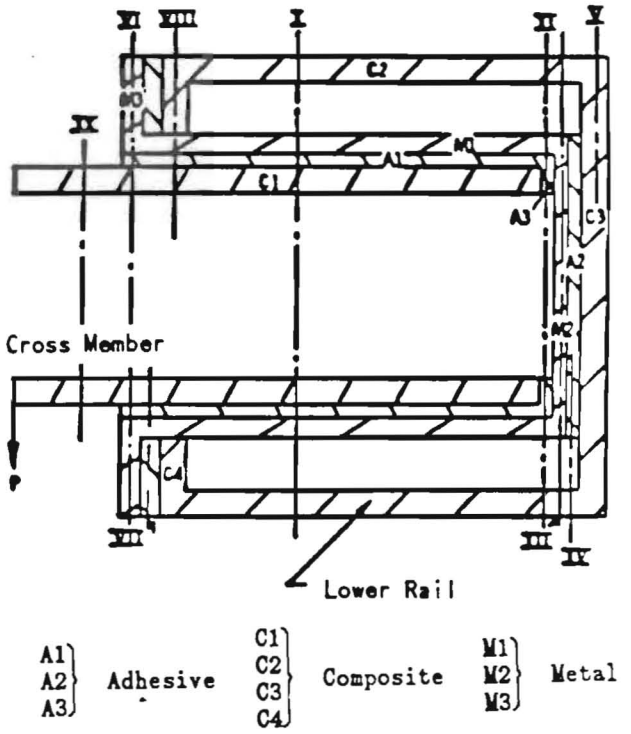

Fig. 3 - Joint Section

Assume a vertical load, P, is applied at the end of the joint. To find the end deflection, δ, apply Castigliano's theorem (based on the energy, U)

$$\delta = \frac{\partial U}{\partial P} . \qquad (1)$$

The energy is obtained from (3)

$$U = \int \frac{M^2}{2EI}\,dx = \int \frac{P^2 x^2}{2EI}\,dx, \qquad (2)$$

where M is the bending moment and EI is the rigidity (product of the modulus of elasticity, E, and the moment of inertia, I) of the cross section. Integrate over the length of the beam for the different sections i and use Eq. (1) to obtain the compliance

$$C = \frac{\delta}{P} = \sum_i \frac{(l_i^3 - l_{i-1}^3)/3}{E_{i-1} I_{i-1}}. \qquad (3)$$

For each section i (e.g. I, II, ..., VIII) the rigidity is found by including the contribution of each material layer κ (composite rail, adhesive, metal insert, etc.),

$$E_i I_i = \sum_\kappa E_\kappa I_\kappa \quad . \qquad (4)$$

Thus a summation is performed across the thickness as well as one lengthwise.

Two additional compliances should be taken into account for the configuration under study (Fig. 3). First, the one due to bending of the lower rail from the load transfer at its midpoint must be considered. In terms of the rigidity $E_1 I_1$ and the length L_{rail} of this bar, this is given by

$$C_1 = 2L^3 / (3E_1 I_1), \quad L_1 = L_{rail}/2 \qquad (5)$$

Second, the compliance due to the torsion of the longitudinal bar should be evaluated. To calculate this quantity, the formulas for thin-walled beams are used. In terms of the mean center line length of the cross section of the lower rail, s, the area enclosed by the mean center line, A_0, the thickness of the lower rail, t_1, its shear modulus, G_1, and the length of the cross member, L_{cm}, the associated torsional deflection at the end of the cross member is

$$\delta_t = \phi L_{cm}, \qquad (6)$$

where the twist angle, ϕ, is obtained from

$$\phi = \tau_t s L_1 / (2A_0 G_1). \qquad (7)$$

In the above expression τ is the torsional shear stress, given by

$$\tau_t = PL_{cm} / (2A_0 t_1). \qquad (8)$$

Thus the total compliance is the sum of the term due to bending of the cross member, the term due to bending of the lower rail, and the term due to torsion of the lower rail.

The shear stress at a position κ of the adhesive is found in terms of the static moment S_κ, the section modulus, $E_s I_s$, and the width w_s, to be

$$\tau_\kappa = \frac{P_s E_\kappa}{E_s I_s w_s} S_\kappa. \qquad (9)$$

In the above formula the subscript s refers to the whole section, whereas the subscript κ refers to the point in question. For full sections P_s is smaller than P. In this case there is shear stress redistribution due to the free edges. To elaborate, consider Figure 4 in which section s consists of subsection s_1 and s_2. To apportion the load at section s_1 use the energy theorem. Assuming M_1, P_{s1} are the moment and load carried by s_1, the energy is expressed as:

$$U = \int \frac{M_{s1}^2}{2E_{s1}I_{s1}}\,dx + \int \frac{(M - M_{s1})^2}{2E_{s2}I_{s2}}\,dx$$

$$= \int \frac{P_{s1}^2 x^2}{2E_{s1}I_{s1}}\,dx + \int \frac{(P - P_{s1})^2 x^2}{2E_{s2} I_{s2}}\,dx. \qquad (10)$$

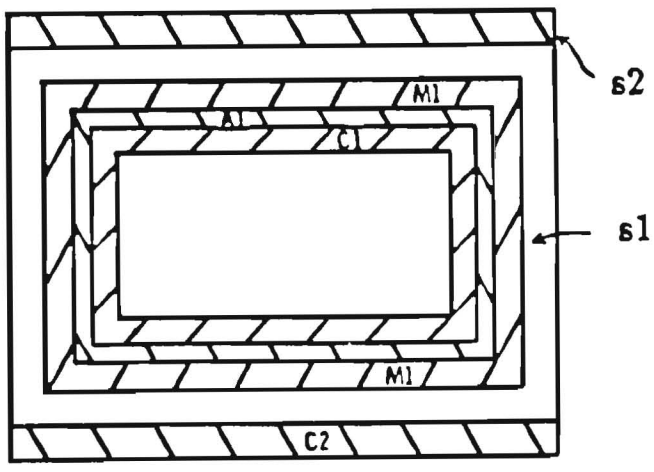

M1 - Metal (aluminum)
C1, C2 - Composite
A1 - Adhesive

Fig. 4 - Section of Joint along Length

Determine P_{s1} by minimizing the energy:

$$\frac{\partial U}{\partial P_{s1}} = 0. \qquad (11)$$

As an example, Figure 3 section I yields:

$$E_{s1}I_{s1} = E_{c1}I_{c1} + E_{m1}I_{m1} + E_{a1}I_{a1}$$

$$E_{s2}I_{s2} = E_{c2}I_{c2}$$

$$P_{s1} = P \frac{E_{s1}I_{s1}}{E_{s1}I_{s1} + E_{s2}I_{s2}}$$

If the geometry were such that a gap were unavoidable, the stresses would increase by a factor of three. The joints in the space frame do not have a gap.

The maximum shear stress occurs at the neutral axis (middle of the cross section). For sections which include the lower rail, the torsion stress τ_t, given by Eq. (8), should be added. It should also be noted that the results indicate the critical shearing stress occurs in the adhesive which bonds the aluminum insert to the lower rail.

The approximate analysis was used to study the effect of changing joint dimensions. Figure 5 illustrates the effect of the aluminum thickness on the shear stress and the insert weight. It can be seen that the aluminum thickness has a moderate effect on the stress but a large effect on the weight. A thickness of 0.3175 cm was selected since it was toward the low weight end and because of material availability.

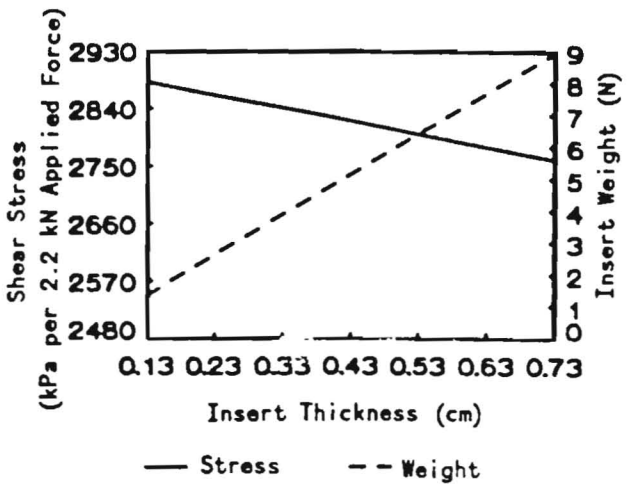

Fig. 5 - Effect of Insert Thickness

Figure 6 shows the effect of the flange width on the flange stress and the insert weight. In this case the flange width largely affects the stress but has a rather moderate effect on the weight.

For the #2 Bar under vertical loading, this approximate formulation predicts the joint stiffness under a 480 N m moment to be 94.6 kN m/rad. The corresponding shear stress, τ, at the middle of the back adhesive is 2850 kPa.

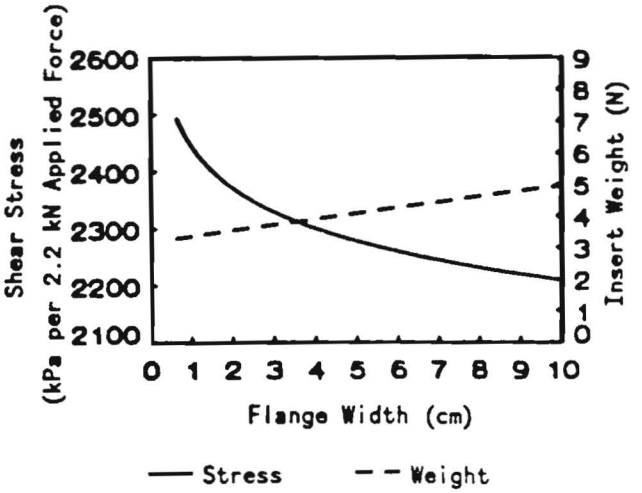

Fig. 6 - Effect of Flange Width

For more details about the stress distribution across the joint, a finite element analysis was performed.

FINITE ELEMENT MODELING PROCEDURES - A detailed finite element model of the T-joint was built using 2800 solid first order isoparametric elements. All materials were modeled including the adhesive. Due to the thin layers of adhesive and aluminum, a large number of elements was necessary to avoid a large aspect ratio. Figure 7 shows a portion of the model used for the analysis, which includes all of the aluminum and adhesive sections. Two elements were used across the aluminum layer and one across the adhesive. The material properties of the Kevlar/epoxy and adhesive are listed in the following table.

Kevlar/epoxy

$E_1 = 53.6$ GPa
$E_2 = 5.0$ GPa
$G_{12} = 2.6$ GPa
$\nu_{12} = 0.34$

Adhesive

$E = 2.8$ GPa
$\nu = 0.25$

A large-deformation elastic stress analysis was completed using the ABAQUS computer code (4). Two different loadings were studied independently

for each joint: a vertical force at the free end of the cross member (P_z in Figure 2) and a force in the fore-aft plane (P_x in Fig. 2). In both cases the maximum stresses were located in the ack adhesive layer that bonds the aluminum nsert to the lower rail.

For the #2 Bar, the more critical service load is in the vertical direction. Therefore, the results in this direction will be discussed

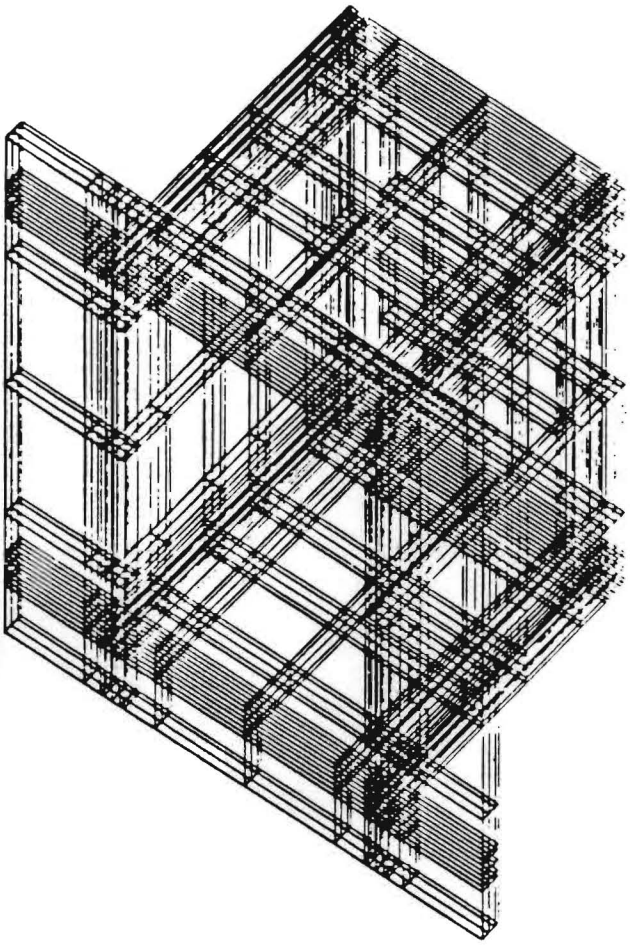

Fig. 7 - Finite Element Model

in detail. A vertical load, P_z, was applied at the end of the cross member producing a moment, M_x, of 480 N m at the joint. The resulting shear and normal stress distributions are shown in Figures 8 and 9, respectively. In Figure 8 the maximum shear stress is at the center which is predicted by beam theory. The corresponding shear stress determined by the energy formulation shown in Fig. 8 is 17% lower than the value found from the finite element analysis.

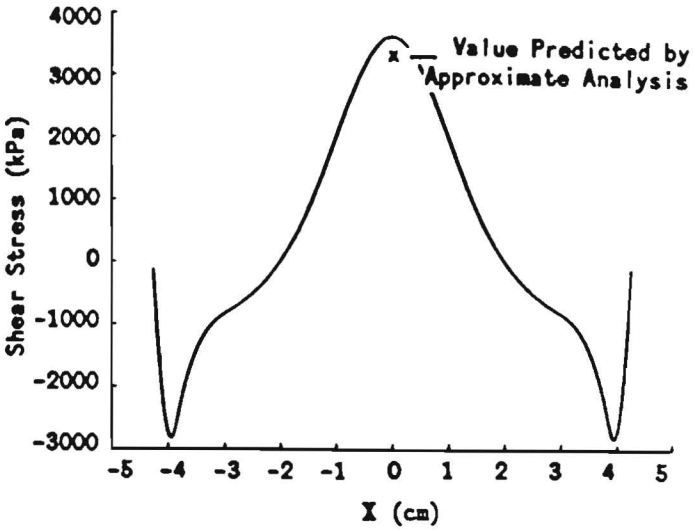

Fig. 8 - Shear Stress Distribution

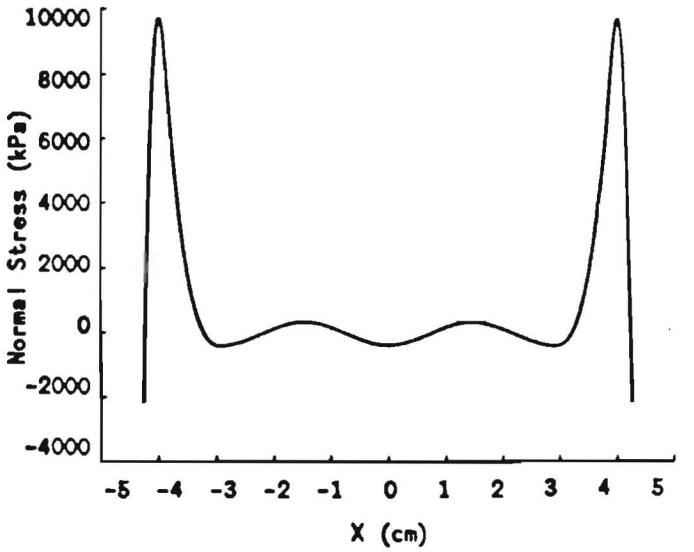

Fig. 9 - Normal Stress Distribution

A similar procedure was followed for each joint design; only the geometry differed. In each case, the maximum stresses in the adhesive do not approach the yield stresses under normal loading conditions.

EXPERIMENTAL PROCEDURES AND VERIFICATION OF RESULTS

The bending tests shown in Figures 10 and 11 are used to verify the results of the analyses and investigate the failure characteristics. Three specimens were tested for each of the three joints under both fore-aft and vertical loading. A strain pot was used to measure displacements at the free end of the cross member where the load was applied.

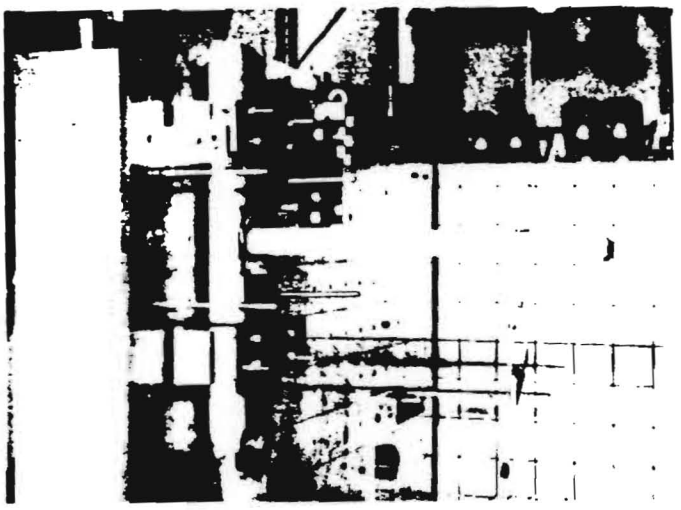

Fig. 10 - Test Configuration for Applying Force P_x

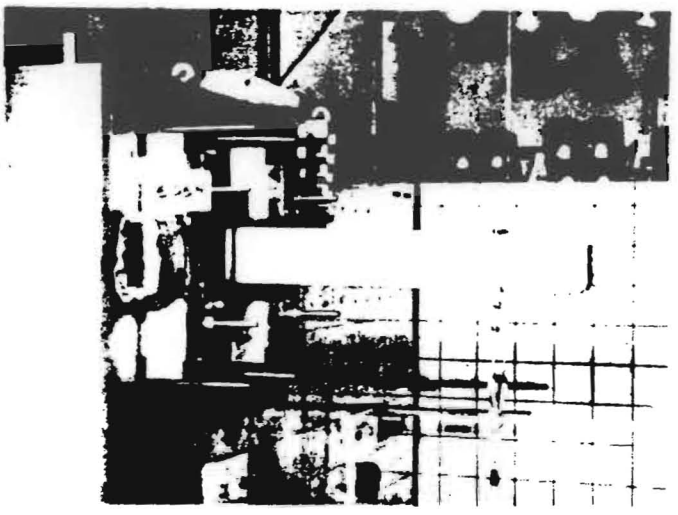

Fig. 11 - Test Configuration for Applying Force P_z

The tests were performed in the elastic range except for the last one for each specimen which was loaded to failure, or, as in most cases, the maximum force the fixture and cable could tolerate. The specimen was hot-melted at each end of the lower rail section to the steel fixture. The whole structure was then bolted to a steel wall. The lower rail was clamped over two inches at each end.

Figure 12 shows the load displacement curves generated for the tests of three specimens of the #2 Bar and the corresponding finite element elastic analysis results. The analysis and the experiments differed by less than 5% in the elastic range. In attempting to fail the joints the maximum moment that could be applied to the #2 bar was over 6 kN m. The experiment was stopped to avoid damaging the fixturing. In the case of the cross member at the engine, the rail was weaker than the joint, and thus, when attempting to load it to failure, the cross member buckled and no damage was done to the joint.

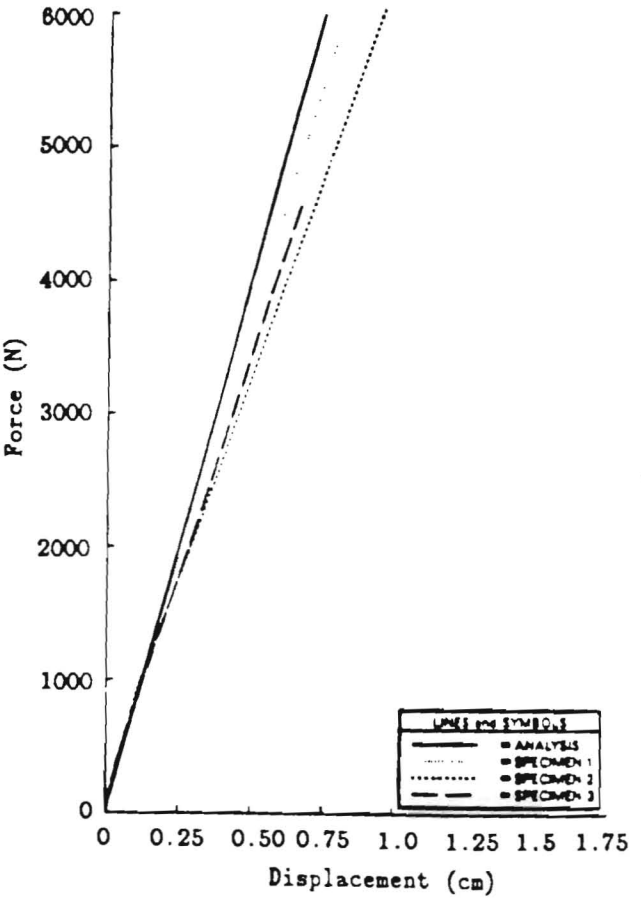

Fig. 12 - Force/Displacement Curves for Tests of the #2 Bar

The joint for the #1 bar cracked in the adhesive layer after applying a moment of 6 kN m to the joint. The crack was located in the adhesive between the flange and the lower rail. It appeared to propagate out from the corner circled in Figure 2. This cohesive failure was predicted by the finite element analysis since this area was shown to have a high stress level.

SUMMARY

Three primary load bearing cross members ttached to the lower rail were analyzed for joint stiffness. A formulation based on the layered beam concept and strain energy theorems was used as an approximate measure to evaluate the relationships between joint flange width, insert thickness, and weight. To obtain additional results regarding the stress distribution throughout the joint, a finite element analysis was completed. Bending tests were used to verify the joint stiffness and determine failure locations. The results from both types of analyses and bending tests are summarized below.

1. The layered beam analysis showed that a larger flange width and thicker aluminum insert reduce the maximum stress in the adhesive but cause a great increase in weight.

2. The results of the finite element analysis and the experiments under both fore-aft and vertical loading differ by at most five percent for the tip deflection of the cross member in the elastic range.

3. Under a 480 N m moment applied to the joint, the effective joint stiffnesses were found to be 23.5, 78.3, and 32.8 kN m/rad under vertical loading, and 10.2, 49.7, and 9.4 kN m/rad under fore/aft loading for the #1 bar, #2 bar, and ross member at the engine, respectively.

ACKNOWLEDGEMENT

The authors wish to thank L. Wickliffe and P. Watling for their help with conducting the experiments.

REFERENCES

1. Adams, R. D. and Wake, W. C., Structural Adhesive Joints in Engineering, Elsevier Applied Science Publishers, New York, 1984.

2. Schmueser, D. W., Wickliffe, L. E., and Mase, G. T., "Front Impact Evaluation of Primary Structural Components of a Composite Space Frame", Conference Proceedings - VII International SAE Vehicle Structural Mechanics Conference, April 11-13, 1988, Detroit, MI.

3. Timoshenko, S., and Young, D. H., Elements of Strength of Materials, D. Van Nostrand Co., 1962.

4. Hibbitt, Karlsson, and Sorensen, "ABAQUS Reference Manuals", May, 1984.